Carbohydrate Polymers 109 (2014) 118–125

Contents lists available at ScienceDirect

Carbohydrate Polymers

journal homepage: www.elsevier.com/locate/carbpol

The improvement of characteristics of biodegradable films made from kefiran–whey protein by nanoparticle incorporation

Mohsen Zolfi [a], Faramarz Khodaiyan [a,*], Mohammad Mousavi [a], Maryam Hashemi [b]

[a] Department of Food Science, Engineering & Technology, Faculty of Agricultural Engineering and Technology, University of Tehran, P.O. Box 4111, Karaj 31587-77871, Iran
[b] Department of Microbial Biotechnology & Biosafety, Agricultural Biotechnology Research Institute of Iran (ABRII), Karaj, Iran

ARTICLE INFO

Article history:
Received 29 January 2014
Received in revised form 24 February 2014
Accepted 2 March 2014
Available online 15 March 2014

Keywords:
Kefiran
Whey protein isolate
Nanoparticles
Biodegradable film
Food packaging

ABSTRACT

Biodegradable kefiran–whey protein isolate (WPI) nanocomposites were produced using montmorillonite (MMT) and nano-TiO_2 as nanoparticles in the percentage of 1, 3, and 5% (w/w) by a casting and solvent-evaporation method. Physical, mechanical, and water-vapor permeability (WVP) properties were determined as a function of nanoparticle concentration. The results revealed that the effect of these nanoparticles was different according to their nature and percentage. The films incorporated with 5% (w/w) MMT showed the highest tensile strength, Young's modulus, puncture strength, and the lowest WVP compared with the control and TiO_2 added films. In contrast to MMT, addition of TiO_2 nanoparticles due to the plasticizing effect led to a significant change in color and transparency of nanocomposite. Scanning electron microscopy (SEM) observations demonstrated the films' properties in relation to their microstructures. The surface topography results also showed a considerable increase in roughness parameters by incorporating the nanoparticles in kefiran–WPI matrix.

1. Introduction

The pollution caused by packaging materials produced from petroleum derivatives, the problems associated with various methods of decontamination such as burying, burning, and recycling them (Tharanathan, 2003), and the hazards related to petroleum-derived raw materials which are used for packaging have led many food researchers to discover and produce natural-based biopolymers that can be used in food packaging (Ghanbarzadeh & Almasi, 2011; Sorrentino, Gorrasi, & Vittoria, 2007). The above-mentioned challenges and concerns are not important in the case of biopolymers, because biodegradation can occur in nature. So, the development of biodegradable materials is an essential need for different societies, and researches on biodegradable materials with controlled properties are an interesting subject for a food specialist (Ghasemlou, Khodaiyan, & Oromiehie, 2011; Gonzalez-Gutierrez, Partal, Garcia-Morales, & Gallegos, 2010).

Whey protein has received much attention for its potential use as a biodegradable film because it has been shown to make transparent films that can act as excellent oxygen barriers and provide certain mechanical properties (Sothornvit, Rhim, & Hong, 2009). Although films produced by whey proteins are good oxygen barriers, they are not an ideal moisture barrier because of the hydrophilic properties of some amino acids present in their structure (Osés, Fabregat-Vázquez, Pedroza-Islas, Tomás, & Cruz-Orea, 2009).

Kefiran, an exopolysaccharide produced by microorganisms present in kefir grains, is a heteropolysaccharide containing glucose and galactose that can be obtained from the grains in high yield when it is produced in deproteinized whey (Ghasemlou, Khodaiyan, & Oromiehie, 2011; Ghasemlou, Khodaiyan, Oromiehie, & Yarmand, 2011a, 2011b; Piermaria, Pinotti, Garcia, & Abraham, 2009). In comparison with other polysaccharides, it has outstanding advantages such as antitumor, antifungal, and antibacterial properties (Cevikbas et al., 1994). In addition, results reported by some researchers showd that kefiran can produce edible films with appropriate appearance and acceptable mechanical properties (Ghasemlou, Khodaiyan, & Oromiehie, 2011; Ghasemlou et al., 2011a, 2011b).

In addition to being capable of degrading biologically, most of the biodegradable polymers have excellent properties that are comparable with those of the petroleum-based plastics, but some properties such as brittleness and high permeability are comparable with gases; this causes their application to be limited. For these reasons, the researches on biopolymers have recently focused on modifying and improving their mechanical and vapor-barrier

* Corresponding author. Tel.: +98 26 3224 8804; fax: +98 26 3224 9453.
E-mail addresses: pardis.ut@gmail.com (M. Zolfi), khodaiyan@ut.ac.ir (F. Khodaiyan).

http://dx.doi.org/10.1016/j.carbpol.2014.03.018
0144-8617/

properties. Introduction of nanotechnology in this field also was one of the most important progresses made recently. Addition of nanoparticles to biopolymers in small amounts improves their mechanical, thermal, and barrier properties and thus can extensively be used for various applications especially food packaging (Avella et al., 2005).

Montmorillonite (MMT) is the most prevalent and important nano-clay that is used. It is because of its favorable properties such as being economical, environmentally friendly, and ease of access that many studies have been conducted on it. This nanoparticle has extensive area and large aspect ratio, so it can act as a filler to effectively strengthen the biopolymers properties (Choi, Kim, Park, Chang, & Lee, 2003).

Titanium dioxide (TiO_2) nanoparticle has been investigated most widely over the past decade because it is cheap, nontoxic, and photostable (Feng et al., 2007). Thin films containing nanosized particles of TiO_2 in their structure exhibit excellent mechanical and chemical stability and can provide a good protection against foodborne microorganisms and allergens in the presence of ultraviolet radiation (Zhou, Wang, & Gunasekaran, 2009). However, there has been no attempt to investigate the incorporation of TiO_2 nanoparticles into biopolymer matrix. Since films produced from biopolymers are very brittle, utilization of good plasticizers is thus inevitable. Polyol plasticizers like glycerol, polyethylene glycol, sorbitol, propylene glycol, and ethylene glycol are usually used in the production of edible and biodegradable films (Ghasemlou, Khodaiyan, & Oromiehie, 2011; Ghasemlou et al., 2011a, 2011b). The aims of this study were to develop a new biodegradable film based on kefiran–WPI with potential applications as a biodegradable film in the food packaging area, and to examine the physical, mechanical, barrier, and microstructural properties of resultant films as a function of nanoparticle type and concentration.

2. Materials and methods

2.1. Materials

Whey protein isolate (WPI, 90 wt% protein) was purchased from Arla Food Ingredient (Tokyo, Japan). Kefir grains, used as starter culture in this study, were obtained from a household in Tehran, Iran. Glycerol and calcium chloride (analytical grade) were purchased from Merck Chemical Co. (Darmstadt, Germany). Sodium chloride was purchased from Dr. Mojallai (Tehran, Iran). Anatase TiO_2 nanoparticles were supplied by Nanoshel LLC (USA). An unmodified natural MMT (Cloisite Na^+) with a density of 2.6 g ml^{-1} was purchased from Southern Clay Products Inc. (Gonzalez, TX).

2.2. Starter culture

Kefir grains were kept in skimmed milk at room temperature for short periods and the medium was renewed daily for new culture to maintain the grains' viability. Seven days after the culture, they were considered active.

2.3. Isolation and purification of kefiran

Exopolysaccharides existing in kefiran grains were extracted by the method of Piermaria et al. (2009) with some modifications (Piermaria et al., 2009). A known amount of kefir grains were stirred in boiling water for one hour. Then, the resultant mixture was centrifuged at 10,000 × *g* for 15 min (Sigma 3-16 k Frankfurt, Germany). To precipitate the secreted polysaccharides, one volume of 96% ethanol was added to the supernatant. The precipitation process of the secreted polysaccharides was carried out at −20 °C for 18 h. Then, in order to separate the precipitated carbohydrate, centrifugation at 10,000 × *g* and 4 °C for 20 min was carried out.

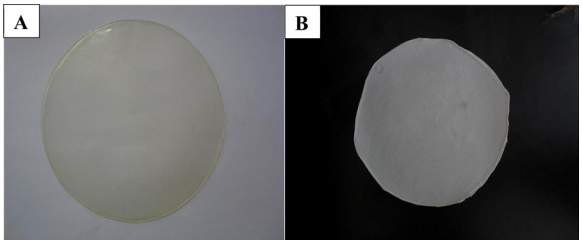

Fig. 1. Illustrative picture of kefiran–WPI biodegradable film containing 5% MMT (A) and 5% TiO_2 (w/w) (B).

The obtained pellet was dissolved in distilled water and again centrifuged under the same conditions. This process was performed three times and the obtained pellet at the end was considered as kefiran.

2.4. Film preparation

A 5% (w/v) WPI solution was prepared by dispersing 5 g of WPI in 100 ml of distilled water and heated in a water-bath at 90 °C for 30 min and then rapidly cooling on ice. Kefiran solution (5%, w/v) was prepared by weighing the amount of film-forming solution under constant magnetic stirring (IKA-WERK, RW 20 DZM, Staufen, Germany) for 15 min. Kefiran–WPI composite films were prepared by mixing equal amount (50:50 (v/v)) of each kefiran and WPI solution. Films prepared without plasticizer were brittle and cracked on the casting plates during drying. Thus, glycerol as plasticizer (35% of total solid weight) was incorporated into the film-forming solution to obtain more flexible films (Ghasemlou et al., 2011a). Following the addition of plasticizer, stirring was continued for a further 15 min. Film solution was transferred into a vacuum oven at 30 °C for 30 min to remove most of the air bubbles incorporated during stirring. On the other hand, MMT was dispersed in distilled water by means of sonication for 1 h at room temperature. The MMT and TiO_2 dispersions were separately added to the aqueous dispersion of kefiran–WPI and stirring was continued for 1 h. In order to have a uniform dispersion of TiO_2 in the kefiran–WPI solution, the addition of TiO_2 was very slow with intense stirring and also with assistance of ultrasound at the same time (Zhou et al., 2009), and stirring was then continued for 1 h. In the next step, about 70 ml of each sample was cast onto the flat, level, non-stick Teflon plates and they were held at room temperature for 18 h to set. Once set, they were peeled off the casting surface and stored in plastic bags inside desiccators at 25 ± 1 °C for further testing (Fig. 1). All treatments were made in triplicate.

2.5. Physical characteristics

2.5.1. Film thickness

The thickness of films was measured using a hand-held micrometer (Alton M820-25, China) with an accuracy of 0.01 mm. The thickness of ten randomly selected points was measured for each testing specimen and the mean value was reported for all experiments.

2.5.2. Transparency

Film transparency was determined by measuring the percentage of transmittance at 600 nm using an UV/vis spectrophotometer (Model 8451A, Hewlett–Packard Co., Santa Alara, CA, USA) (Rhim, Hong, Park, & Ng, 2006).

2.5.3. Colorimetric measurements

The color characteristics of films were determined using a colorimeter (Colorflex CX1542, USA). Film specimens were placed

on a white standard plate (L^* = 96.9, a^* = −0.33 and b^* = 0.16) and the lightness (L) and, chromaticity parameters a (red–green) and b (yellow–blue) were triplicately measured. L-Values were in the range of 0 (black) to 100 (white); a values ranges from −80 (greenness) to 100 (redness); and b values ranges from −80 (blueness) to 70 (yellowness). The total color difference (ΔE) and whiteness index (WI) were calculated using Eqs. (1) and (2), respectively (Ghasemlou et al., 2011a):

$$\Delta E = \sqrt{(L^* - L)^2 + (a^* - a)^2 (b^* - b)^2} \quad (1)$$

$$WI = 100 - \sqrt{(100 - L)^2 + a^2 + b^2} \quad (2)$$

where L^*, a^*, and b^* are the color parameter values of the standard and L, a, and b are the color parameter values of the sample.

2.6. Mechanical properties

Tensile strength (TS), elongation at break (EB), Young's modulus (YM), puncture strength (PS) and puncture deformation (PD) were evaluated using a Machine M350-10CT (Testometric Co., Ltd., Rochdale, Lancs., England) according to the ASTM standard method D882-02 (ASTM, 1995). The films were cut in rectangular strips of 100 mm in length and 10 mm in width. All the specimens were kept in a desiccator of 50 ± 5% relative humidity (RH) using saturated calcium nitrate solution for 48 h. Films were fixed with an initial grip separation of 50 mm and stretched at a cross-head speed of 10 mm min^{-1}. Three replicates were run for each film specimen.

For puncture test, three specimens (discs of 3 cm diameter) were cut from the each pre-conditioned sample. Each disc was mounted on the top of a test cup and a smooth-edged cylindrical probe (2 mm in diameter) was moved perpendicularly onto the film surface at a cross-head speed of 10 mm min^{-1} until the film broke. Force-deformation data collected by a microcomputer were used to determine the PS and PD of the film at rupture.

2.7. Water-vapor permeability measurements

The films' water vapor permeability (WVP) was gravimetrically measured according to the standard method E96 (ASTM, 1995) and corrected for the stagnant air gap inside test cups (Gennadios, Weller, & Gooding, 1994). The film was sealed onto a glass permeation cup (mouth area 1.25×10^{-4} m^2) containing silica gel (desiccant RH 0%) with an O-ring to hold the film in place. The cups were then placed in a desiccator equilibrated at 25 °C and 75% RH with saturated sodium chloride solution. The cups were weighed at certain intervals, and a linear regression analysis of weight gain versus time was performed. The slopes of the steady state (linear) portion of weight loss versus time curves were used to calculate water vapor transmission rate (WVTR). The WVP coefficient was calculated according to:

$$WVP = \frac{WVTR \times X}{\Delta P} \text{ (g/m s Pa)} \quad (3)$$

where ΔP is the vapor partial pressure difference across the film (Pa) and X is film thickness (m).

2.8. Scanning electron microscopy

Scanning electron microscopy (SEM) measurements were carried out by a scanning electron microscope (Oxford Instruments INCA Penta FET × X3). The samples were fractured in liquid nitrogen, mounted on aluminum stubs using a double-sided adhesive tape, and sputtered with a thin layer of gold using a BAL-TEC SCD 005 sputter coater (BALTEC AG, Balzers, Liechtenstein). All samples were examined using an accelerating beam at a voltage of 15 kV. Samples were photographed at an angle of 90° to the surface to allow observation of the films' cross-section.

2.9. Atomic-force microscopy

Atomic-force microscopy (AFM; Dualscope/Rasterscope C26, DME, Denmark) was used to study surface morphology of the film samples that had been previously equilibrated at atmosphere with RH of 50%. Film specimens were cut into thin pieces that could be fit into AFM imaging, and double-sided tape was used to stick them onto the sample stage. All film samples were scanned in noncontact mode. A sharpened cantilever with a spring constant of 25 N/m was positioned over the samples, and 50 μm × 50 μm images were obtained. For each sample, the results were transformed into 3D images (Fabra, Talens, & Chiralt, 2009). To make comparable results, all images were obtained from the center area of each surface. Dualscope/Rasterscope SPM software (Version 2.1.1.2) was used to calculate the roughness value of the films. Different roughness parameters can be also measured by AFM. Some of these parameters are reported in this study (Eqs. (4)–(6)) (Khulbe, Feng, & Matsuura, 2008).

S_a is the average roughness evaluated over the complete surface, and is defined as:

$$S_a = \int \int_a |Z(x, y)| \cdot dx \cdot dy \quad (4)$$

where Z is the height function of the area.

S_q is the root mean square (RMS) of roughness expressed as follows:

$$S_q = \sqrt{\int \int_a |Z(x, y)|^2 \cdot dx \cdot dy} \quad (5)$$

S_{dq} (RMS gradient) defines the slope for each point of area excluding points on the edge and is calculated as follows:

$$S_{dq} = \sqrt{\frac{1}{A} \int_0^x \int_0^y \left(\left(\frac{\partial Z(x, y)}{\partial x} \right)^2 + \left(\frac{\partial Z(x, y)}{\partial y} \right)^2 \right) \cdot dx \cdot dy} \quad (6)$$

2.10. Statistical analysis

Statistics on a completely randomized design were performed with the analysis of variance (ANOVA) procedure using SPSS software (Version 11.5; SPSS Inc., Chicago, USA). Duncan's multiple range tests were used to compare the difference among mean values of film specimens' characteristics at a statistical level of 0.05.

3. Results and discussion

3.1. Thickness

As considered in Fig. 2A, the thickness of kefiran–WPI films is about 0.074 mm. The results indicated that addition of both nanoparticles increased the thickness of films as a result of their incorporation in the polymer matrix, but amount of this increase differed for each nanoparticle. TiO_2 did not have great influence on the thickness because of its nature and small diameter, whereas MMT significantly increased the thickness of films ($p < 0.05$), so that the thickness of film by adding 5% MMT reached to 0.091 mm. According to their laminated structure, MMT expands and the space between layers becomes larger when it comes into contacts with solvent (Petersson & Oksman, 2006), thus it was expected to have a greater increase in thickness.

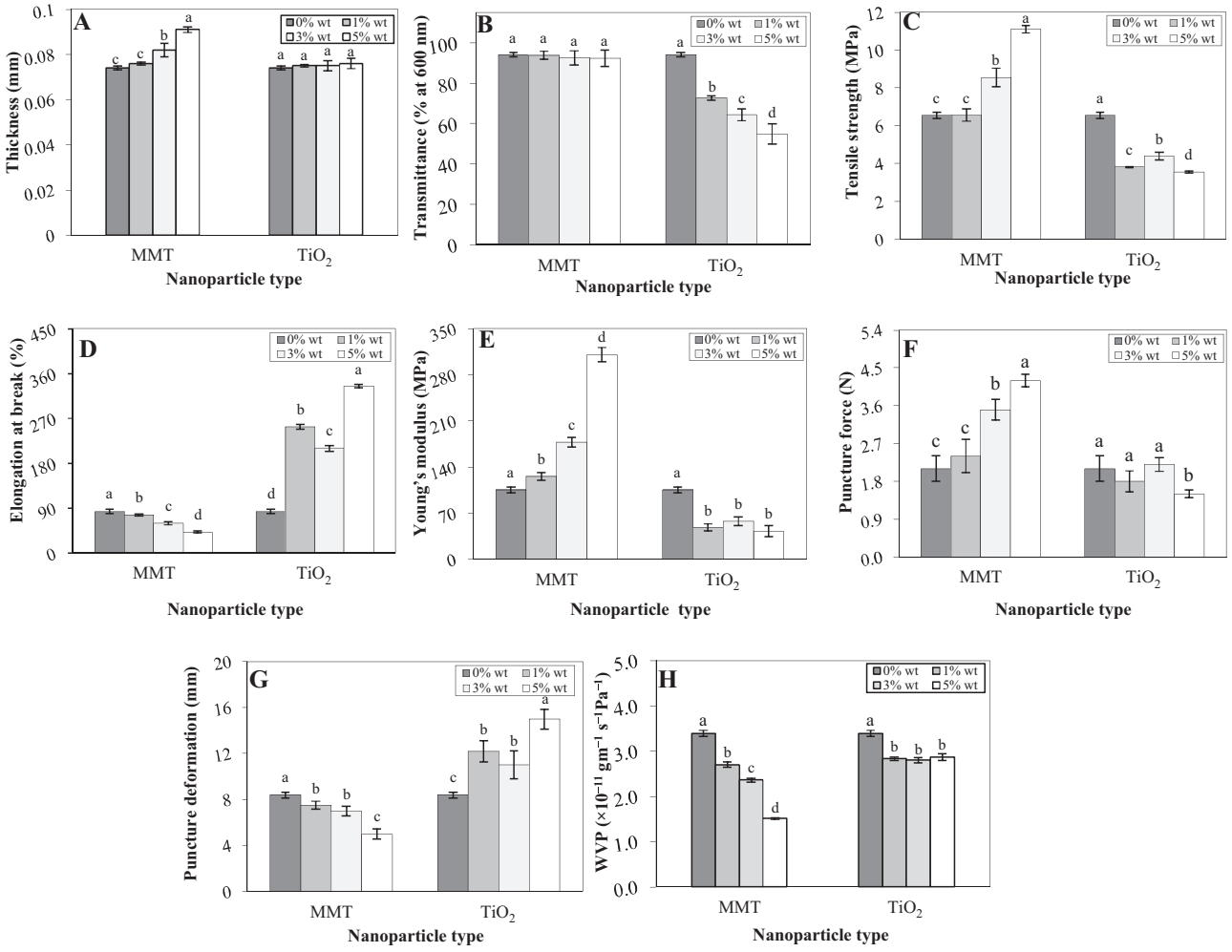

Fig. 2. Effect of nanoparticle level and type on the thickness (A), transparency (B), WVP (C), TS (D), EB (E), YM (F), PS (G) and PD (H) of kefiran–WPI films. Columns with the same letter are not significantly different ($p < 0.05$).

The thickness of films will have an ascending pattern by increasing the percentage of nanoparticle into both nanocomposite films, but for nanocomposites containing TiO_2 it was negligible (Fig. 2A).

3.2. Transparency

Transparency is one of the important features of films that affect its application and also it is an index that indicates mixing capability of polymer mixture without losing its properties (Piermaria et al., 2009; Tang, Zou, Xiong, & Tang, 2008). Maintaining the nanocomposites transparency after addition of nanoparticle, with respect to initial polymer, is a key parameter that should be taken into account during the nanocomposites preparation. The transparency measurements showed that kefiran–WPI films have a high transparency (≈93.99%), while it had a slight alteration after the MMT adding (Fig. 2B). This low decrease indicates complete distribution of MMT into polymer matrix. Since most of the nanoparticles have dimensions smaller than wavelength of visible waves, it is expected that by exfoliation of nanoparticles especially MMT in the polymer matrix, sensible changes will not be observed in the transparency of films (Zeng, Yu, Lu, & Paul, 2005).

Transparency of composite kefiran–WPI films significantly decreased ($p < 0.05$) after adding of TiO_2 as this decrease was dependent on the amount of nanoparticle. Thus, the transparency reached to a minimum level (54.85%) at concentration of 5% TiO_2 nanoparticle (Fig. 2B). This behavior can be probably due to non-uniform distribution of nanoparticles. The microscopic images also show recognizable agglomeration of them in the level of 5%, but nanoparticles distribution is uniform at level of 1 and 3%. An increase in crystallinity and a decrease in amorphous regions in structure of films could be also expectable. The metallic nature of TiO_2 is also responsible for this behavior as the authors observed a white solution during preparation of films and during mixing of this nanoparticle in water. So, the latter reason is the more likely one.

3.3. Color attributes

Film color is an important property in the acceptability of product by consumer. The parameters of L (lightness), a (green–red), b (blue–yellow), ΔE (difference between color of white plate and samples), and WI (whiteness index) values are shown in Table 1. Generally, a decrease in L- and a-value and an increase in factor of b were observed by adding MMT. However, decrease of the L-value was not significant (Table 1) which can be due to the hydrophilic property of MMT and its compatibility with hydrophilic biopolymers of kefiran and whey proteins (Sothornvit et al., 2009). Also, the adding of MMT also increased ΔE value and decreased WI index ($p < 0.05$).

The L-value was significantly increased by adding TiO_2 to the polymer as from 83.45 for kefiran–WPI films where it reached to 95.72 for those containing 5% TiO_2 ($p < 0.05$). Also, the factors of a,

Table 1
Hunter color values (L, a, and b), total color difference (ΔE) and whiteness index (WI) of kefiran–WPI films as a function of MMT and TiO_2 concentration.

Film samples	Color attributes[a,b]				
	L	a	b	ΔE	WI
Kefiran–WPI	83.45 ± 1.21^{d}	-0.54 ± 0.82^{a}	9.91 ± 0.28^{c}	16.81 ± 1.17^{d}	80.68 ± 1.10^{d}
Kefiran–WPI–1% MMT	82.91 ± 1.56^{d}	-0.81 ± 0.60^{ab}	12.50 ± 1.38^{b}	18.73 ± 1.37^{c}	78.76 ± 1.56^{e}
Kefiran–WPI–3% MMT	82.58 ± 2.15^{d}	-1.16 ± 0.57^{b}	13.09 ± 1.30^{b}	20.34 ± 1.76^{b}	77.23 ± 1.88^{e}
Kefiran–WPI–5% MMT	82.08 ± 2.50^{d}	-1.58 ± 0.51^{c}	15.00 ± 0.44^{a}	22.59 ± 1.80^{a}	75.07 ± 1.64^{f}
Kefiran–WPI–1% TiO_2	90.09 ± 1.51^{c}	-0.90 ± 0.70^{ab}	9.53 ± 0.96^{c}	12.04 ± 1.40^{e}	86.06 ± 1.33^{c}
Kefiran–WPI–3% TiO_2	93.60 ± 1.17^{b}	-1.10 ± 0.48^{b}	8.00 ± 1.15^{c}	9.09 ± 0.86^{f}	89.54 ± 1.20^{b}
Kefiran–WPI–5% TiO_2	95.72 ± 1.95^{a}	-1.31 ± 0.56^{bc}	6.80 ± 0.63^{d}	7.19 ± 1.16^{g}	91.96 ± 1.10^{a}

[a] Means within each column with same letters are not significantly different ($p < 0.05$).
[b] Data are means ± SD.

b, and ΔE decreased by adding TiO_2, whereas the WI was increased (Table 1).

Most decrease in the a-value was observed in nanocomposites containing MMT. This fact indicates that greenness in resultant nanocomposites has increased, while there is a decrease in their redness.

3.4. Mechanical properties

The results of mechanical parameters of produced films in terms of TS, EB, YM, PD, and PS in RH of 50% and temperature of 25 °C are shown in Fig. 2C–G. The TS, YM and EB values for kefiran–WPI film were 6.54 MPa, 105.33 MPa, and 83.79%, respectively. TS and YM levels of the different films considerably increased by the MMT addition but their EB was significantly decreased. An increase in TS and YM values could be due to the change in layers orientation and the increase in layers resistance, aspect ratio and surface area by exerting MMT nanoparticles (Cyras, Manfredi, Ton-That, & Vázquez, 2008) and homogenous distribution of these nanoparticles in the polymer matrix (Sothornvit et al., 2009; Xu, Ren, & Hanna, 2005).

It should be noted that the TS value will not increase by any increase in MMT content because the probability of exfoliation of MMT in nanocomposite film is reduced at higher concentrations of the nanoparticle. On the other hand, agglomeration of the nanoparticles at high amounts by increasing attractive forces between them in the matrix is known to occur (Xu et al., 2005). TiO_2 unlike MMT showed a different behavior, TiO_2 distribution between the kefiran–WPI chains due to its nature and spherical shape led to a reduction in polymer cross-links and thus increased the mobility. As illustrated in Fig. 2C–E, the TS, EB and YM values of nanocomposites containing 1% TiO_2 were of 3.8, 48.1 MPa, and 253.5%, respectively. The TS and YM showed an increase by increasing nanoparticle up to 3%, but the EB value was decreased. This fact

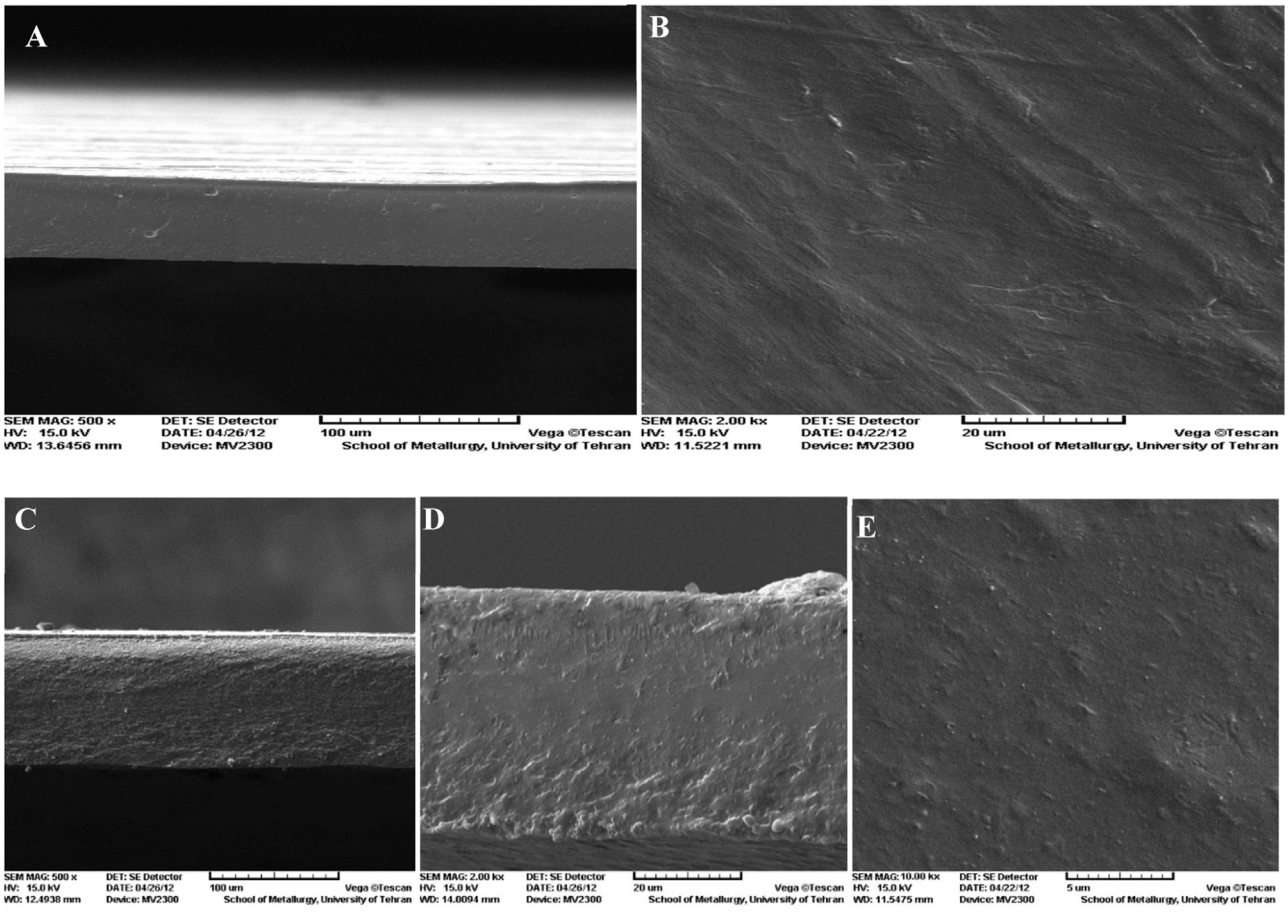

Fig. 3. SEM micrographs of surfaces (B, E) and fracture surface (A, C and D) of kefiran–WPI (A and B), and kefiran–WPI–5% wt MMT nanocomposites (C–E).

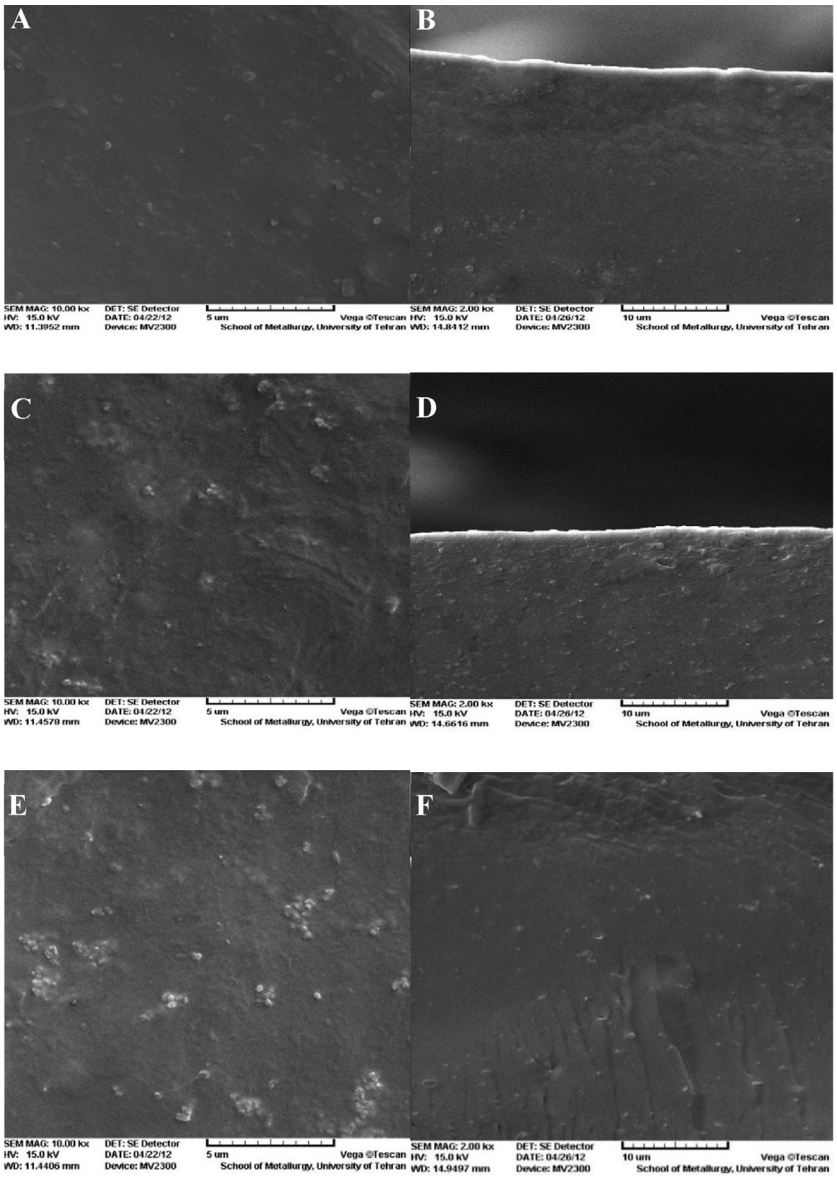

Fig. 4. SEM micrographs of surface (A, C and E) and fracture surfaces (B, D and F) of kefiran–WPI nanocomposites containing 1% (A and B), 3% (C, D) and 5% (E and F) TiO_2.

can be related to the more compact structure of these nanocomposites compared to those containing 1 and 5% TiO_2. Then, the values of TS and EB by increasing the amount of nanoparticle up to 5%, reduced due to the nanoparticle agglomeration. This assumption can be confirmed by the SEM images.

Fig. 2F shows that the PS of composite film by adding MMT to kefiran–WPI solution increased compared with kefiran–WPI film. Unlike MMT, the PS value by increasing the nano-TiO_2 content from 1 to 5% was decreased from 1.82 to 1.51 mm. As earlier described, this was due to the differences in structure, the number of active hydroxyl groups, nanoparticles type and some other properties in the nanocomposite film matrix.

3.5. Water vapor permeability

Since one of the most important applications of food packages is reducing the transfer of moisture between food and its surrounding atmosphere, the WVP of packaging materials should be at the minimum (Zhou et al., 2009).

The WVP results of different samples showed that this character was decreased by adding the nanoparticles (MMT and TiO_2), especially at high concentrations (Fig. 2H). The WVP for kefiran–WPI was about 3.39×10^{-11} g m^{-1} S^{-1} Pa^{-1} that shows the relatively weak barrier property of this biopolymer to water vapor. This value by addition of 5% MMT, decreased to 1.51×10^{-11} g m^{-1} S^{-1} Pa^{-1}.

A decrease of 20.35–55.45% in WVP values of nanocomposites containing different concentrations of MMT could be due to the impermeable silicate layers with large aspect ratio that are completely distributed in the polymer matrix (Sothornvit, Hong, An, & Rhim, 2010) and make a tortuous path for diffusing molecules. So in order to cross the film thickness, these molecules should turn around these sheets and the distance and time of effective diffusion will be increased and thus permeability is consequently reduced (Kumar, Sandeep, Alavi, Truong, & Gorga, 2010). Moreover, It can easily distribute within polymer matrix and can improve its impermeability to water vapor because of hydrophilic nature of MMT and its compatibility with hydrophylic kefiran–WPI biopolymers (Sothornvit et al., 2009).

The WVP results of TiO_2 nanocomposites showed that the permeability by addition of this nanoparticle is insignificantly reduced ($p > 0.05$). The WVP value was reduced to 2.8×10^{-11} g m^{-1} S^{-1} Pa^{-1}

Table 2
The roughness parameters obtained from atomic force microscopy images.[a]

Film samples	Roughness parameters		
	S_a (nm)	S_q (nm)	S_{dq}
Kefiran–WPI	150.00 ± 3.50[c]	200.50 ± 2.32[c]	0.082 ± 0.022[c]
Kefiran–WPI–5% TiO_2	215.20 ± 4.08[b]	281.00 ± 4.24[b]	0.158 ± 0.019[b]
Kefiran–WPI–5% MMT	233.50 ± 4.53[a]	307.90 ± 2.12[a]	0.171 ± 0.007[a]

[a] Values (mean and standard deviation) within each column followed by different letters indicate significant differences ($p < 0.05$).

by increasing the concentration of TiO_2 up to 3% and then reached to 2.87×10^{-11} g m^{-1} S^{-1} Pa^{-1} for the samples containig 5% TiO_2. However, this value was still lower than permeability of kefiran–WPI films.

Negligible effect of TiO_2 on the reduction of WVP (about 17.40%) can be due to small aspect ratio of this nanoparticle and the chains disorder increase. Zhou et al. (2009) reported that nanoparticles with large aspect ratio like alumina (Al_2O_3) and MMT show a significant reduction in WVP of nanocomposites. Owing to increase of plasticizing and disordely characteristics by adding TiO_2 nanoparticles, it was expected that permeability would increase, but results obtained in this work were vice versa. The possible reason for this phenomenon can be because of increased hydrophobicity of TiO_2 nanoparticles compared to WPI and kefiran molecules (Zhou et al., 2009).

3.6. SEM microstructure characteristics

The obtained microstructures on surface of kefiran–WPI and its nanocomposites using SEM analysis are shown in Figs. 2 and 3. As it is seen, kefiran–WPI film had a smooth and even surface without crack and bubble (Fig. 3A and B). Addition of MMT nanoparticles to kefiran–WPI film led to a compact and tortuous structure that can very well prevent the molecular diffusion. Since MMT nanaoparticles have been homogeneously distributed into biopolymer matrix (Fig. 3C–E), the structure of films was not destroyed by increasing the MMT amounts. The obtained results were in agreement with the findings of Rhim et al. (2006), and Casariego et al. (2009).

Micrographs obtained from the samples containing TiO_2 also showed that they had a granular structure (Fig. 4). There is no considerable agglomeration at the concentrations of 1–3% TiO_2. This fact indicates a good distribution for these nanoparticles in the polymeric structure. However, a high agglomeration was observed at the concentration of 5% TiO_2 (Fig. 4). These results were similar to those found by Zhou et al. (2009), who investigated the influence of TiO_2 on the properties of WPI films.

3.7. Surface topography

AFM is a powerful tool to study structure and different surfaces of polymers. It has been used to provide qualitative (the morphology) and quantitative (the roughness) information about biopolymers at a nanometer scale that could not usually be obtained by any other experimental technique. AFM has been previously used to study isolate edible films (Bergo, Sobral, & Prison, 2010). In Table 2, the results of topographical assessment of kefiran–WPI and nanocomposites containing 5% MMT and TiO_2 are shown. As considered in this table, three main parameters of roughness such as S_a, S_q and S_{dq} were compared. Three dimensional images of these nanocomposites surfaces are also shown in Fig. 5. The obtained results indicate significant differences ($p < 0.05$) in all three parameters between the different samples. The S_a, S_q, and S_{dq} values for kefiran–WPI film were 150 nm, 200.5 nm, and 0.082, respectively. It is seen that all three parameters by addition of 5% nanoparticles to the polymer matrix had an ascending behavior. The increase in the surface roughness was principally

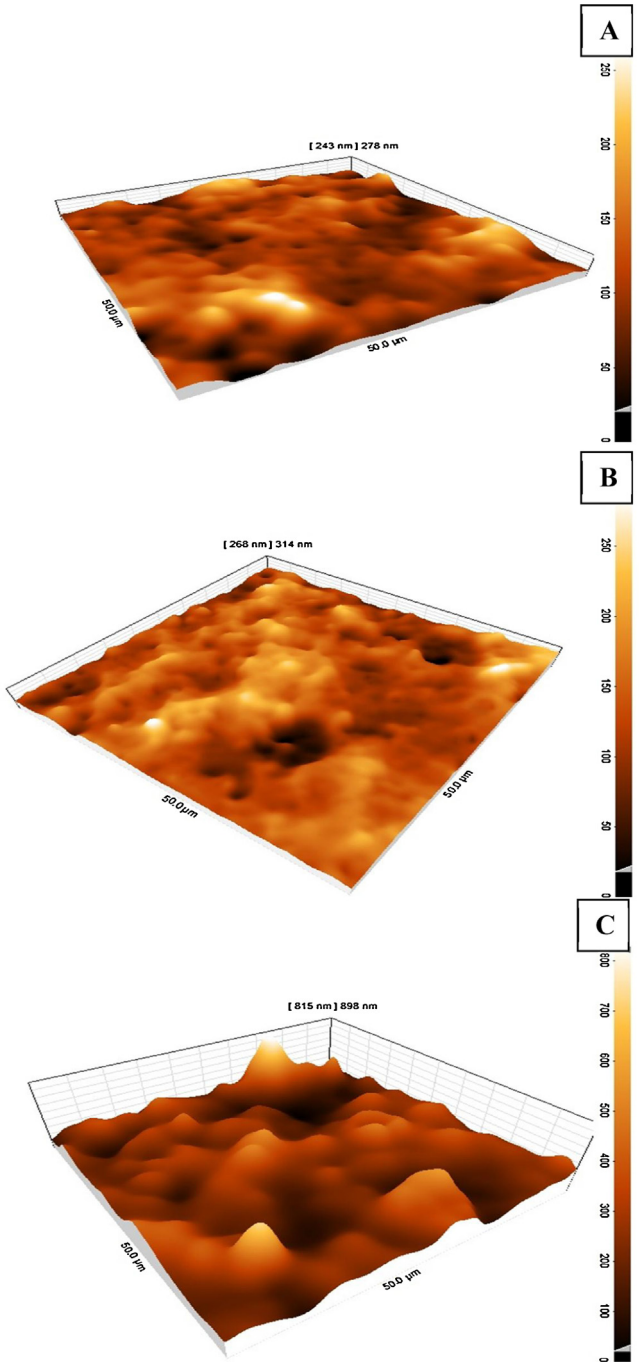

Fig. 5. AFM topographic images of kefiran–WPI (A), kefiran–WPI–5% TiO_2 (B) and kefiran–WPI–5% MMT (C).

due to the mixture of nanoparticles in the structure of composite films. Also, 3D images of these nanocomposites clearly show these changes (Fig. 5). The kefiran–WPI film had a smooth surface, while the nanocomposite containing TiO_2 compared to this film showed more ridges. However, the nanocomposite containing MMT had the highest projections (Fig. 5).

4. Conclusion

In this study, bionanocomposite films were developed based on kefiran–WPI with different amounts of MMT and TiO_2 nanoparticles using the casting method. The results showed that the properties of these films were greatly influenced by MMT and nano-TiO_2 content. Incorporation of MMT into the polymeric matrix by improving the physical and mechanical properties provides a compact structure that can significantly decrease the WVP of films. The TS and YM values increased by increasing MMT concentration, while EB value of these films significantly decreased. TiO_2 as a metalic nanoparticle, after addition to the polymeric matrix, changed the color attributes and increased the transperancy of nanocomposites. The TS value because of increase in the disorderness and mobility of polymer chains were decreased by adding this nanoparticle, while the EB significantly increased. This fact revealed that TiO_2 had a quasi-placticizing role for kefiran–WPI films. It seems that biodegradable kefiran–WPI–MMT nanocomposites have great potential in the food packaging applications for long-time storage.

Acknowledgements

The authors wish to express their gratitude to University of Tehran for supporting the facilities for this research work and technical assistance.

References

ASTM. (1995). Standard test methods for water vapor transmission of material. In *Annual book of ASTM*. Philadelphia: American Society for Testing and Materials.

Avella, M., de Vlieger, J. J., Errico, M. E., Fischer, S., Vacca, P., & Volpe, M. G. (2005). Biodegradable starch/clay nanocomposite films for food packaging applications. *Food Chemistry*, *93*, 467–474.

Bergo, P., Sobral, P. J. A., & Prison, J. M. (2010). Effect of glycerol on physical properties of cassava starch films. *Journal of Food Processing and Preservation*, *34*, 401–410.

Casariego, A., Souza, B., Cerqueira, M., Teixeira, L., Diaz, R., & Vicente, A. (2009). Chitosan/clay films' properties as affected by biopolymer and clay micro/nanoparticles concentrations. *Food Hydrocolloids*, *23*(7), 1895–2190.

Cevikbas, A., Yemni, E., Ezzedenn, F. W., Yardimici, T., Cevikbas, U., & Stohs, S. J. (1994). Antitumoural, antibacterial and antifungal activities of kefir and kefir grains. *Phytotherapy Research*, *8*, 78–82.

Choi, W. M., Kim, T. W., Park, O. O., Chang, Y. K., & Lee, J. W. (2003). Preparation and characterization of poly (hydroxybutyrate-co-hydroxyvalerate)–organoclay nanocomposites. *Journal of Applied Polymer Science*, *90*, 525–529.

Cyras, V. P., Manfredi, L. B., Ton-That, M. T., & Vázquez, A. (2008). Physical and mechanical properties of thermoplastic starch/montmorillonite nanocomposite films. *Carbohydrate Polymers*, *73*, 55–63.

Fabra, M. J., Talens, P., & Chiralt, A. (2009). Microstructure and optical properties of sodium caseinate films containing oleic acid–beeswax mixtures. *Food Hydrocolloids*, *23*, 676–683.

Feng, X. X., Zhang, L. L., Chen, J. Y., Guo, Y. H., Zhang, H. P., & Jia, C. I. (2007). Preparation and characterization of novel nanocomposite films formed from silk fibroin and nano-TiO_2. *International Journal of Biological Macromolecules*, *40*, 105–111.

Gennadios, A., Weller, C., & Gooding, C. (1994). Measurement errors in water vapor permeability of highly permeable, hydrophilic edible films. *Journal of Food Engineering*, *21*, 395–409.

Ghanbarzadeh, B., & Almasi, H. (2011). Physical properties of edible emulsified films based on carboxymethyl cellulose and oleic acid. *International Journal of Biological Macromolecules*, *48*, 44–49.

Ghasemlou, M., Khodaiyan, F., & Oromiehie, A. (2011). Physical, mechanical, barrier, and thermal properties of polyol-plasticized biodegradable edible film made from kefiran. *Carbohydrate Polymers*, *84*, 477–483.

Ghasemlou, M., Khodaiyan, F., Oromiehie, A., & Yarmand, M. S. (2011a). Development and characterisation of a new biodegradable edible film made from kefiran, an exopolysaccharide obtained from kefir grains. *Food Chemistry*, *127*, 1496–1502.

Ghasemlou, M., Khodaiyan, F., Oromiehie, A., & Yarmand, M. S. (2011b). Characterization of edible emulsified films with low affinity to water based on kefiran and oleic acid. *International Journal of Biological Macromolecules*, *49*, 378–384.

Gonzalez-Gutierrez, J., Partal, P., Garcia-Morales, M., & Gallegos, C. (2010). Development of highly-transparent protein/starch-based bioplastics. *Bioresource Technology*, *101*, 2007–2013.

Khulbe, K. C., Feng, C., & Matsuura, T. (2008). *Synthetic polymeric membranes: Characterization by atomic force microscopy*. Germany: Springer.

Kumar, P., Sandeep, K. P., Alavi, S., Truong, V. D., & Gorga, R. E. (2010). Preparation and characterization of bio-nanocomposite films based on soy protein isolate and montmorillonite using melt extrusion. *Journal of Food Engineering*, *100*, 480–489.

Osés, J., Fabregat-Vázquez, M., Pedroza-Islas, R., Tomás, A. S., & Cruz-Orea, A. (2009). Development and characterization of composite edible films based on whey protein isolate and mesquite gum. *Journal of Food Engineering*, *92*, 56–62.

Petersson, L., & Oksman, K. (2006). Biopolymer based nanocomposites: Comparing layered silicates and microcrystalline cellulose as nanoreinforcement. *Composites Science and Technology*, *66*, 2187–2196.

Piermaria, J. A., Pinotti, A., Garcia, M. A., & Abraham, A. G. (2009). Films based on kefiran, an exopolysaccharide obtained from kefir grain: Development and characterization. *Food Hydrocolloids*, *23*, 684–690.

Rhim, J., Hong, S., Park, H., & Ng, P. (2006). Preparation and characterization of chitosan-based nanocomposite films with antimicrobial activity. *Journal of Agriculture and Food Chemistry*, *54*, 5814–5822.

Sorrentino, A., Gorrasi, G., & Vittoria, V. (2007). Potential perspectives of bionanocomposites for food packaging applications. *Trends in Food Science & Technology*, *18*, 84–95.

Sothornvit, R., Hong, S. I., An, D. J., & Rhim, J. W. (2010). Effect of clay content on the physical and antimicrobial properties of whey protein isolate/organo-clay composite films. *LWT – Food Science and Technology*, *43*, 279–284.

Sothornvit, R., Rhim, J. W., & Hong, S. I. (2009). Effect of nano-clay type on the physical and antimicrobial properties of whey protein isolate/clay composite films. *Journal of Food Engineering*, *91*, 468–473.

Tang, S., Zou, P., Xiong, H., & Tang, H. (2008). Effect of nano-SiO_2 on the performance of starch/polyvinyl alcohol blend films. *Carbohydrate Polymers*, *72*, 521–526.

Tharanathan, R. N. (2003). Biodegradable films and composite coatings: Past, present and future. *Food Science and Technology*, *14*, 71–78.

Xu, Y., Ren, X., & Hanna, M. A. (2005). Chitosan/clay nanocomposite film preparation and characterization. *Journal of Applied polymer Science*, *99*, 1684–1691.

Zeng, Q. H., Yu, A. B., Lu, G. Q., & Paul, D. R. (2005). Clay-based polymer nanocomposites: Research and commercial development. *Journal of Nanoscience and Nanotechnology*, *5*, 1574–1592.

Zhou, J. J., Wang, S. Y., & Gunasekaran, S. (2009). Preparation and characterization of whey protein film incorporated with TiO_2 nanoparticles. *Journal of Food Science*, *74*, 50–55.